

Meso/Macroporous, Mechanically Stable Silica Monoliths of Complex Shape by Controlled Fusion of Mesoporous Spherical Particles

Petr O. Vasiliev, Zhijian Shen, Robert P. Hodgkins, and Lennart Bergström*

Materials Chemistry Research Group, Department of Physical, Inorganic and Structural Chemistry, Arrhenius Laboratory, Stockholm University, SE-106 91 Stockholm, Sweden

Received May 23, 2006. Revised Manuscript Received July 31, 2006

The fabrication of meso/macroporous monoliths by partial fusion of mesoporous silica spheres with the use of the pulsed current processing (PCP) method was demonstrated. Mesoporous silica spheres have been prepared by evaporation-driven surfactant templating in microdroplets. The PCP method can simultaneously subject powder bodies to a rapid temperature increase and a compressive stress. By keeping the fusing temperature low, it was possible to form a continuous body where the particles were connected by necks formed at the surface of the particles, while the mesoporous structure was retained within the particles. The structure, porosity, necking, and mechanical properties of the fused mesoporous particles are strongly dependent on the applied pressure and temperature. This novel approach allows for flexible and independent tailoring of the bimodal pore structure together with rapid production of mechanically stable monoliths of arbitrary shape and is of interest in various applications, e.g., as membranes, sensors, catalyst support, slow-release agents, chromatography, and groundwater treatment.

Introduction

The synthesis and processing of porous materials are of interest for many applications, e.g., catalysis, separation technology, sensors, and chromatography.^{1–3} Pore engineering, i.e., how to control and tailor the pore size and connectivity over a wide range of length scales, is the key to obtaining materials with optimum performance. With the relatively recent development of surfactant-templated inorganic mesoporous materials with well-defined pores on the nanometer scale,^{4–7} we now have tools to tailor pore sizes from ångströms up to micrometers and millimeters. Hierarchically porous materials, specifically, materials that possess well-defined macropores and interconnected meso- and/or micropores, have attracted much interest, as these materials are expected to be superior to monomodal porous materials for many applications.

There are a multitude of approaches to synthesizing materials that display a multiscale porosity. The use of self-assembling surfactants or block-copolymers in conjunction with other larger scale structure-directing agents, e.g., polymeric colloids,^{8–11} microemulsions,¹² air bubbles,¹³ and

starch granules,¹⁴ to direct the structure during assembly, gelation, and polymerization of inorganic species have resulted in bimodally porous materials. Recent work has shown that by carefully selecting the self-assembling agents and controlling the synthesis conditions, it is even possible to prepare hierarchically porous silica materials on three distinct length scales.^{15,16} Other approaches involving controlled phase separation in parallel with the sol–gel transition of the inorganic precursor^{17–19} or hydrothermal transformation of arrays of silicalite-coated mesoporous particles²⁰ have also been successful in creating hierarchically porous materials.

Despite the significant progress in synthesizing hierarchically porous materials, the preparation of such materials with a well-defined macroscopic shape and significant mechanical strength in a rapid and facile manner remains a challenge.

* To whom correspondence should be addressed. E-mail: Lennartb@inorg.su.se. Tel.: 46 8 16 23 68. Fax: 46 8 15 21 87.

(1) Davis, M. E. *Nature* **2002**, *417*, 813.

(2) Stein, A. *Adv. Mater.* **2003**, *15*, 763.

(3) Antonietti, M.; Ozin, G. A. *Chem.—Eur. J.* **2004**, *10*, 29.

(4) Beck, J. S.; Vartuli, J. C.; Roth, W. J.; Leonowicz, M. E.; Kresge, C. T.; Schmitt, K. D.; Chu, C. T. W.; Olson, D. H.; Sheppard, E. W.; McCullen, S. B.; Higgins, J. B.; Schlenker, J. L. *J. Am. Chem. Soc.* **1992**, *114*, 10834.

(5) Kresge, C. T.; Leonowicz, M. E.; Roth, W. J.; Vartuli, J. C.; Beck, J. S. *Nature* **1992**, *359*, 710.

(6) Zhao, D. Y.; Feng, J. L.; Huo, Q. S.; Melosh, N.; Fredrickson, G. H.; Chmelka, B. F.; Stucky, G. D. *Science* **1998**, *279*, 548.

(7) Yanagisawa, T.; Shimizu, T.; Kuroda, K.; Kato, C. *Bull. Chem. Soc. Jpn.* **1990**, *63*, 988.

(8) Antonietti, M.; Berton, B.; Goltner, C.; Hentze, H. P. *Adv. Mater.* **1998**, *10*, 154.

(9) Yin, J. S.; Wang, Z. L. *Appl. Phys. Lett.* **1999**, *74*, 2629.

(10) Lebeau, B.; Fowler, C. E.; Mann, S.; Farcet, C.; Charleux, B.; Sanchez, C. *J. Mater. Chem.* **2000**, *10*, 2105.

(11) Rhodes, K. H.; Davis, S. A.; Caruso, F.; Zhang, B. J.; Mann, S. *Chem. Mater.* **2000**, *12*, 2832.

(12) Schmidt-Winkel, P.; Lukens, W. W.; Yang, P. D.; Margolese, D. I.; Lettow, J. S.; Ying, J. Y.; Stucky, G. D. *Chem. Mater.* **2000**, *12*, 686.

(13) Bagshaw, S. A. *Chem. Commun.* **1999**, *9*, 767.

(14) Zhang, B. J.; Davis, S. A.; Mann, S. *Chem. Mater.* **2002**, *14*, 1369.

(15) Kuang, D. B.; Brezesinski, T.; Smarsly, B. J. *Am. Chem. Soc.* **2004**, *126*, 10534.

(16) Sen, T.; Tiddy, G. J. T.; Casci, J. L.; Anderson, M. W. *Angew. Chem., Int. Ed.* **2003**, *42*, 4649.

(17) Amatani, T.; Nakanishi, K.; Hirao, K.; Kodaira, T. *Chem. Mater.* **2005**, *17*, 2114.

(18) Ishizuka, N.; Minakuchi, H.; Nakanishi, K.; Soga, N.; Tanaka, N. *J. Chromatogr., A* **1998**, *797*, 133.

(19) Kanamori, K.; Yonezawa, H.; Nakanishi, K.; Hirao, K.; Jinnai, H. *J. Sep. Sci.* **2004**, *27*, 874.

(20) Dong, A. A.; Wang, Y. J.; Tang, Y.; Zhang, Y. H.; Ren, N.; Gao, Z. *Adv. Mater.* **2002**, *14*, 1506.

Previous work has involved the use of, for example, a molded polystyrene foam with a tailored structure that serves as a macroporous scaffold for the mesostructure-forming sol-gel/amphiphilic block-copolymer composite.²¹ Plastic forming of a gel consisting of mesostructured nanoparticles can yield monoliths of various shapes with disordered bimodal pore structures.²² Polymerization of a monomer solution in a concentrated suspension of mesoporous particles has been used to make bimodally porous silica columns for chromatography.²³ Småt et al. illustrated how hierarchically porous silica monoliths of simple shapes could be prepared by carefully controlling the phase separation and gelation kinetics in conjunction with surfactant templating in a mold.²⁴ All these previous reports use solution-based techniques to control the pore structure and prepare the monoliths. Removal of large amounts of solvent from large object with a high porosity and small pore sizes is very time-consuming, with processing times usually on the order of several days. The capillary-induced drying stresses often lead to significant shrinkage and can result in cracking and warpage.

In the present work, we introduce a rapid and facile approach that adopts the convenience and flexibility of powder-based processes used in, for example, the ceramic field²⁵ to produce mechanically stable meso/macroporous monoliths of complex shape. Mesoporous spherical particles produced by an aerosol-assisted technique have been assembled in a die and rapidly consolidated into a monolith. It is shown how the surface area, mechanical strength, and macroscopic shape of the bimodally porous monolith can be tailored. The mechanism of the formation of strong interparticle bonds is discussed, and the independent tailoring of the mesopore and macropore sizes is demonstrated.

Experimental Section

Two types of surfactant-templated mesoporous spheres produced by aerosol assisted techniques displayed a narrow pore size distribution, controlled by the templating amphiphilic molecule, but varied in the particle size distribution. The majority of the work was performed using polydisperse spheres with a pore size of 96 Å, produced by a modified spraying technique²⁶ by the Institute for Surface Chemistry (YKI). The triblock copolymer of Pluronics series (BASF) P123, EO₂₀P₇₀EO₂₀, was used as the templating amphiphilic molecules and the droplet formation of the copolymer/sol-gel solution was performed in a two-fluid spray nozzle (Pneumatic atomizer). The as-prepared P123-templated polydisperse spherical silica particles were rendered porous after calcination at 550 °C for 4 h in air to remove remaining organics.

Mesoporous monodisperse spheres with a smaller pore size of 21 Å have been prepared in monodisperse droplets of surfactant and prehydrolyzed silica solution generated by an aerosol generator

VOAG (TSI Model 3450), essentially following ref 27. The precursor solution was prepared by mixing a prehydrolyzed solution of 10.4 g of tetraethoxysilane, TEOS (Purum >98%), in 5.4 g of diluted hydrochloric acid (pH 2) and 12 g of ethanol (99.7%) under vigorous stirring at room temperature for 20 min. The cationic surfactant hexadecyl trimethylammonium bromide, C₁₆TAB, Aldrich, was used as the templating amphiphilic molecule; 3.2 g of C₁₆TAB was dissolved in 62 g of ethanol (99.7%) before being mixed with the prehydrolyzed TEOS solution. The operation of the aerosol generator is based on the instability and break up of a cylindrical liquid jet via a vibrating orifice (20 μm) into uniform droplets. A pump syringe (velocity ≈ 1.3 × 10⁻³ cm/s) forces the mixture through the vibrating orifice, employing a frequency of 70–80 kHz at a constant amplitude. By careful control of the frequency and amplitude, the liquid jet can be tailored to give a steady stream of monodispersed droplets while simultaneously suppressing the evolution of satellite droplets. The droplets were injected axially from the vibrating orifice with a turbulent dispersion air jet (~15 cm³/min) to suppress any coalescence of particles followed by a greater volume of a lamellar flow of dilution air (~40 L/min) into a vertical drying chamber (10 cm diameter), where evaporation of solvents takes place. The silica skeleton was condensed by passing the particles through a stainless steel tube (4 cm diameter) inside of a three-zone furnace at 250 °C (calibrated with thermocouples) before the particles were collected at a filter (Pall, A/D Glass fiber filter, with diameter 4.7 mm). The CTAB-templated monodisperse particles were calcined at 550 °C for 4 h in air to remove the surfactant template.

Hierarchically meso/macroporous monoliths have been fabricated by partial fusion of the mesoporous powder in a vacuum in a pulsed current processing apparatus (Dr. Sinter 2050, Sumitomo Coal Mining Co. LTD, Japan). The calcined mesoporous powders were loaded in cylindrical, dome- and prism-shaped graphite dies and fused with an uniaxial pressure of 20 MPa at a heating rate of 100 °C/min. The temperature was regulated by a thermocouple that was inserted into the pressing graphite die.

Shaping of the hierarchically porous monoliths was performed by simple machining using a thin cutting wheel and driller mounted on a pneumatic cutter.

Characterization of the mesoporous particles and the hierarchically porous monoliths was carried out using different methods. Scanning electron microscopy (SEM) micrographs were obtained via a JEOL 820 microscope operating at 10 keV. Samples were thinly spread onto a carbon film supported on a brass stud. HRTEM micrographs were taken using a JEOL JEM-200 FX-II microscope operating at 200 keV and equipped with a CCD camera. Samples were ground before being dispersed in ethanol and then deposited onto a carbon film supported on a Cu grid.

Porosity measurements were obtained volumetrically using a micromeritics ASAP 2020 analyzer. Samples were degassed and data collection started at typically 77 K, following a program consisting of both an adsorption and desorption branch. The specific surface areas were calculated using the BET model within $p/p^\circ = 0.08$ – 0.3 relative pressure region. The mesopore size distributions were obtained from the analysis of the adsorption branch via the nonlocal density functional theory (NLDFT),²⁸ with the assumption of cylindrical pore geometry.

The macropore volume and the pore size distribution of hierarchically porous monoliths were determined using mercury intrusion porosimetry (Micromeritics AutoPore III 9410). The determination is performed within the pore diameter interval 120

- (21) Maekawa, H.; Esquena, J.; Bishop, S.; Solans, C.; Chmelka, B. F. *Adv. Mater.* **2003**, *15*, 591.
- (22) El Haskouri, J.; de Zarate, D. O.; Guillem, C.; LaTorre, J.; Caldes, M.; Beltran, A.; Beltran, D.; Descalzo, A. B.; Rodriguez-Lopez, G.; Martinez-Manez, R.; Marcos, M. D.; Amoros, P. *Chem. Commun.* **2002**, *4*, 330.
- (23) Liang, C. D.; Dai, S.; Guiochon, G. *Chem. Commun.* **2002**, *22*, 2680.
- (24) Småt, J. H.; Schunk, S.; Linden, M. *Chem. Mater.* **2003**, *15*, 2354.
- (25) Ring, T. A. In *Fundamentals of Ceramic Powder Processing and Synthesis*; Academic Press: San Diego, 1996; Chapter 17.
- (26) Andersson, N.; Alberius, P. C. A.; Pedersen, J. S.; Bergstrom, L. *Microporous Mesoporous Mater.* **2004**, *72*, 175.

- (27) Rao, G. V. R.; Lopez, G. P.; Bravo, J.; Pham, H.; Datye, A. K.; Xu, H. F.; Ward, T. L. *Adv. Mater.* **2002**, *14*, 1301.
- (28) Ravikovitch, P. I.; Neimark, A. V. *J. Phys. Chem. B* **2001**, *105*, 6817.

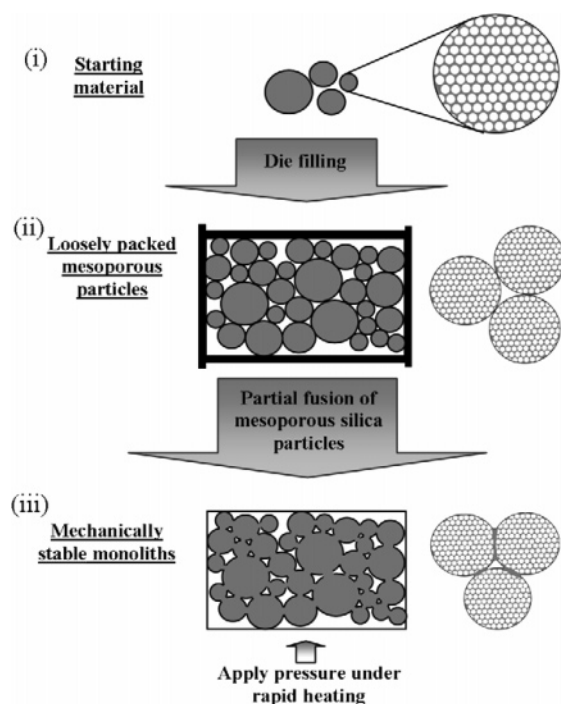


Figure 1. Schematic illustration of the process used to prepare bimodal porous monoliths from mesoporous particles.

$\mu\text{m} \geq \Phi \geq 100 \text{ \AA}$. The surface tension and the contact angle of mercury are set to 485 mN/m and 130° , respectively.

The diametral compression test, also known as the Brazilian test or splitting tensile test, of the cylindrical monoliths was performed by applying a compressive load on the perimeter of the circular disk until a crack forms, causing failure of the specimen. Diametral compression tests were carried out at ambient conditions using an electromechanical testing machine (Zwick Z050, Germany) at a constant cross-head displacement rate of 0.5 mm/min. The test specimens were subjected to diametral compression using two parallel plates. Tensile strength is calculated as $\sigma_T = 2P/(\pi dt)$, where P = load at failure (N), d = specimen diameter (mm) and t = specimen thickness (mm).

Results and Discussion

The integrated process for producing mechanically stable meso/macroporous monoliths of complex shape is schematically illustrated in Figure 1. The process involves three steps, namely (i) synthesizing mesoporous particles; (ii) assembling the particles in a die with a designed shape; and (iii) subjecting the powder assembly to a compressive stress and simultaneously rapidly heating the powder body to a temperature where amorphous silica can be viscoelastically deformed. This treatment induces a partial fusion of the mesoporous particles at the contact point.

The partial fusion technique of mesoporous particles yields monoliths that exactly replicate the shape of the fabrication die, e.g., cylindrical, dome-shaped, and square-shaped (Figure 2a). Problems with shrinkage and cracking that often plague solution-based methods are insignificant, and it is possible to manufacture large objects in a short time. The total process time from loading the die with the powder and removing the monoliths is less than 30 min, and the size of the object is basically limited by the size of the die. The obtained monoliths have bimodal pore structures, which consist of

mesopores with a well-defined long-range order and interconnected, disordered macropores that are a result of the interstices between the partially fused particles (Figure 2b,c). The size of the intergranular macropores is mainly determined by the size and packing of the mesoporous particles prior to and during the heating sequence, whereas the structure of the intragranular mesopores essentially remains unaffected by the partial fusion process and is thus controlled by the conditions set in the particle synthesis step, i.e., the molecular structure and concentration of the amphiphilic template. This novel approach provides the advantages of flexible tailoring of the bimodal pore structure together with very rapid production of strong monoliths with complex geometry.

The use of rapid heating in conjunction with an applied compressive stress is essential for the production of strong hierarchically porous monoliths with a minimal distortion and collapse of the internal mesostructure of the mesoporous powders. Conventional techniques to form a monolith from a powder assembly by, for example, pressureless sintering requires a mass transport to the contact points to form the solid necks that provide the strength of the material.²⁹ The mass transport is thermodynamically driven by the minimization of surface free energy; hence, when mesoporous powder body is subjected to heat, there is a competition between the reduction of the internal and external surface areas. Heating an assembly of a mesoporous powder with a high internal surface area for an extended time, as reported, for example, by Liang et al.,²³ may result in a weakly bonded monolith, but it will be difficult to create a strong monolith without substantially compromising the internal pore structure. In contrast, the pulsed current processing (PCP) method,²⁹ where the rapid temperature increase is created by the electrical current that is passed through the graphite die and the powder assembly, can create a relatively large area of contact between the mesoporous particles with a minimal mass transport. The high stress at the contact points at temperatures above 650°C results in a viscoelastic deformation of the amorphous silica framework. It is well-known that this type of amorphous, glasslike material (on the atomic length-scale) exhibit a time-dependent deformation behavior, also below the glass transition point.^{30,31} Figure 2b suggests that heating to 700°C results in the formation of a contact zone that is relatively large without distorting the initial mesostructure inside the particles. Increasing the temperature to 800°C results in a larger deformation of the particles that also appears to distort the mesostructure, at least in the region close to the deformation zone, Figure 2c.

Evaporation-assisted self-assembly of an amphiphilic template, e.g., a nonionic surfactant of the Pluronic family, or a cationic surfactant like cetyltrimethylammonium bromide (CTAB) and hydrolyzed TEOS in an aerosol can create spherical powders with a range of particle sizes and internal structures.^{26,27,32–35} We have used two types of mesoporous

(29) Shen, Z.; Nygren, M. *Chem. Rec.* **2005**, 5, 173.

(30) Scherer, G. W. *Relaxation in Glass and Composites*; Wiley: New York, 1986.

(31) Sakai, M.; Shimizu, S.; Ito, S. *J. Am. Ceram. Soc.* **2002**, 85, 1210.

(32) Lu, Y. F.; Fan, H. Y.; Stump, A.; Ward, T. L.; Rieker, T.; Brinker, C. J. *Nature* **1999**, 398, 223.

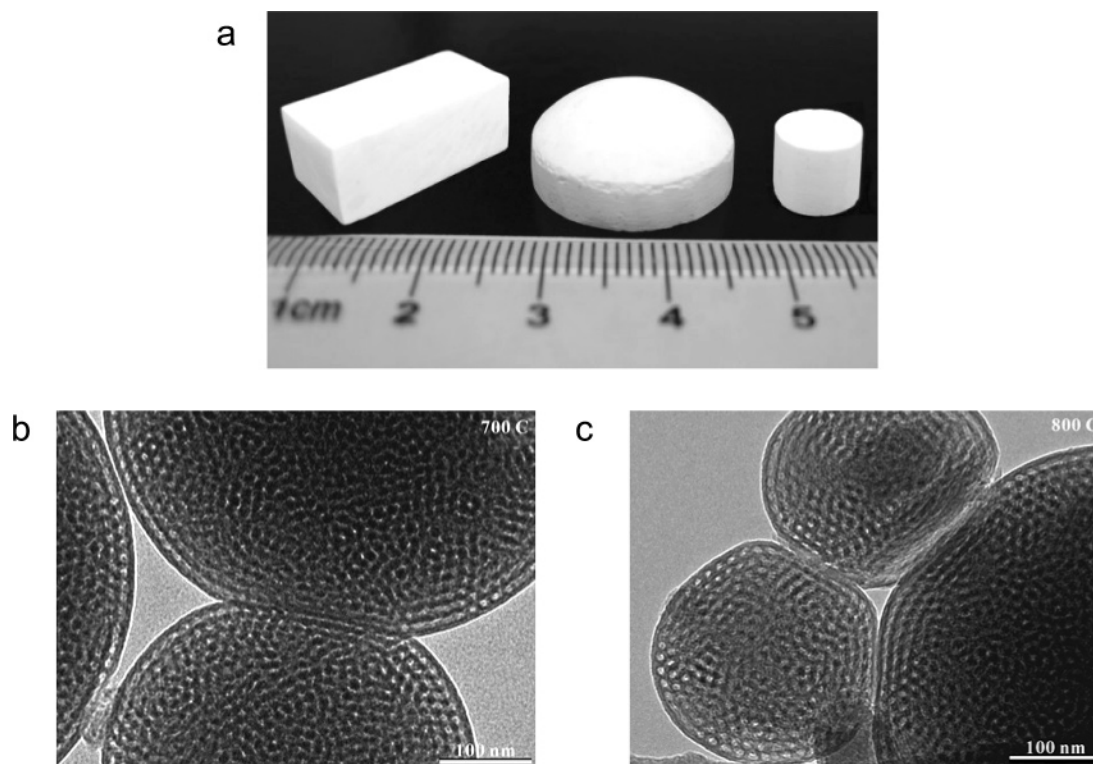


Figure 2. (a) Meso/macroporous silica monoliths of different shapes prepared by rapid heating of an assembly of mesoporous particles in dies of different shapes (700 °C, 20 MPa); (b and c) TEM images of the deformed contact zone of the of the P123-templated, polydisperse mesoporous silica particles, subjected to 20 MPa applied pressure and rapid heating to 700 and 800 °C, respectively.

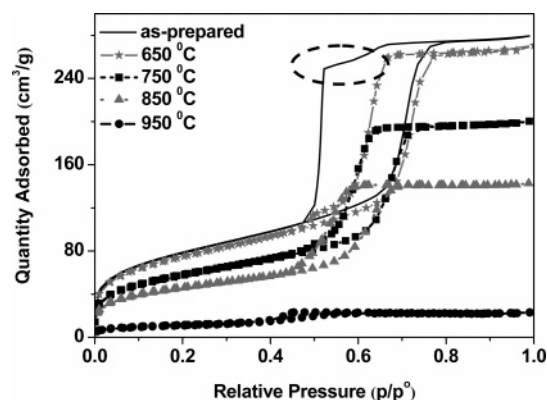


Figure 3. N₂ adsorption-desorption isotherms of as-prepared and partially fused P123-templated, polydisperse mesoporous silica particles at temperatures between 650 and 950 °C.

powders in this study. The major part of the work is completed on the basis of polydisperse P123-templated mesoporous silica spheres produced by a recently reported spraying technique that can produce relatively large quantities of mesostructured particles with a well-defined internal structure.²⁶ These particles have a two-dimensional hexagonal symmetry with a uniform mesoporous structure and are polydisperse, with a typical size distribution between 0.5 and 5 μm . Monodispersed mesoporous particles with a diameter of 12 μm have also been produced using a vibrating orifice

Table 1. Porosity and Tensile Strength of Meso/Macroporous Monoliths Produced by Partial Fusion of P123-Templated, Polydisperse Particles at Different Temperatures

T_{max} (°C)	specific surface area BET ^a (m ² /g)	total mesopore volume ^b (cm ³ /g)	total macropore volume (cm ³ /g)	mesopore diameter ^d (Å)	tensile strength ^e (MPa)
1050	2.28	0.0015	<0.01		
1000	2.56	0.003			23.8
950	38	0.035	0.18		
900	147	0.191		75	7.4
850	159	0.219	0.19	75	
800	191	0.296		75	1.6
750	202	0.307	0.26	82	
700	239	0.368		96	0.8
650	261	0.411	0.32	96	
as-made	275	0.429		96	

^a BET surface area calculated within $p/p^0 = 0.08-0.3$. ^b Single-point adsorption total pore volume at relative pressure $p/p^0 = 0.96$ for pores <508 Å. ^c Macropore volume for all pores with a diameter >0.1 μm . ^d Mesopore diameters were determined by the NLDFT. ^e Tensile strength was obtained from diametral compression of cylindrical monoliths.

aerosol generator that can produce precursor droplets with a very narrow size distribution.²⁷

The N₂ adsorption-desorption isotherms (Figure 3) are typical for mesoporous solids with cylindrical pore geometry. There is a wide hysteresis for the untreated particles (shown by an oval in Figure 3), which gradually disappears with increasing temperature in the PCP process. We speculate that the wide hysteresis originates from a fraction of lamellar pores near the surface of the as-made particles.²⁶ Subjecting the powder assembly to a high temperature and pressure creates a deformation of the particles at the contact points (Figure 2b,c), which could reduce the fraction of lamellar pores and thus explain why the wide hysteresis disappears with increasing process temperature. The pore size of the

(33) Bore, M. T.; Rathod, S. B.; Ward, T. L.; Datye, A. K. *Langmuir* **2003**, *19*, 256.

(34) Grosso, D.; Illia, G.; Crepaldi, E. L.; Charleux, B.; Sanchez, C. *Adv. Funct. Mater.* **2003**, *13*, 37.

(35) Bruinsma, P. J.; Kim, A. Y.; Liu, J.; Baskaran, S. *Chem. Mater.* **1997**, *9*, 2507.

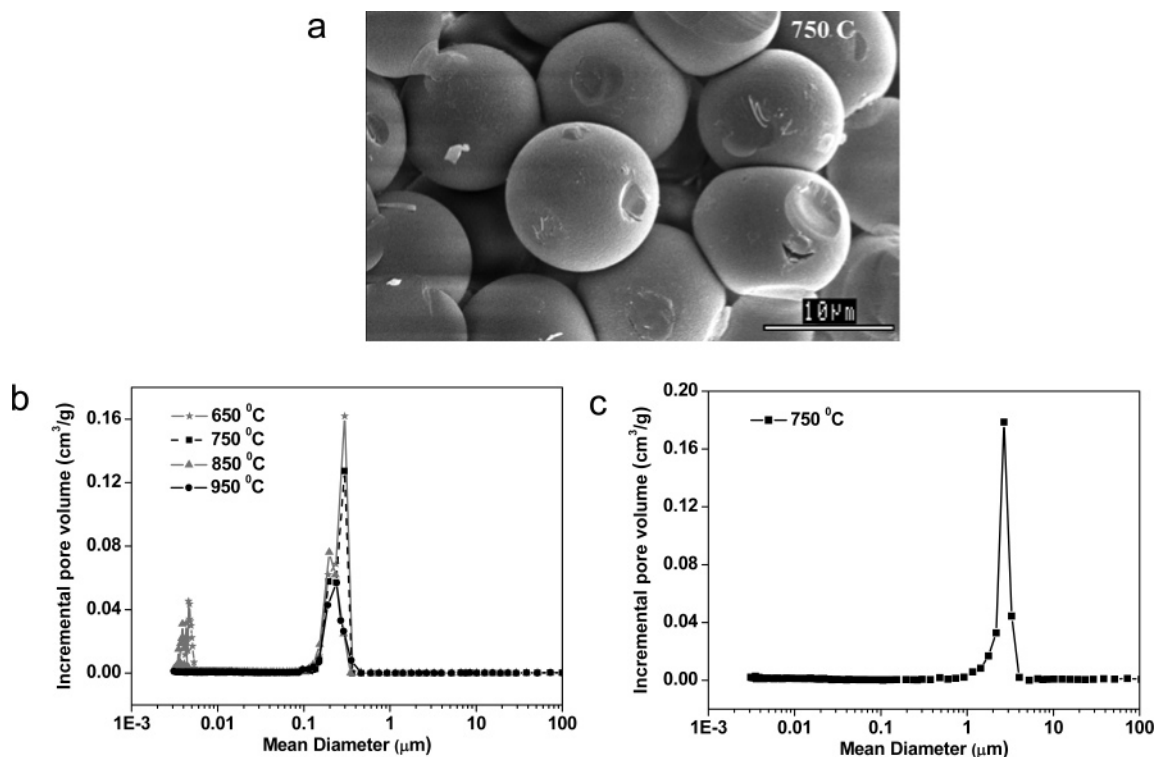


Figure 4. (a) Scanning electron microscopy image of monodisperse CTAB-templated mesoporous particles after partial fusion at 750 °C at an applied pressure of 20 MPa. Mercury intrusion porosimetry data of monoliths prepared from rapidly heated assemblies of (b) P123-templated, polydisperse and (c) CTAB-templated, monodisperse mesoporous silica particles, respectively, at an applied pressure of 20 MPa; note that the mesoporosity of the CTAB-templated particles in c is too small (21 Å) for mercury to penetrate.

calcined P123-templated particles of 96 Å is retained in the monoliths fused up to 700 °C (Table 1). There is a slight reduction in the pore size to 82 and 75 Å for the monoliths fused at 750 and 800 °C, respectively, but the size distribution is still narrow. In contrast, both the specific surface area and the volume of the mesopores decrease with an increase in the fusion temperature (Table 1). The decrease appears to be essentially linear up to 950 °C, where the mesostructure eventually collapses. This suggests that the viscoelastic deformation at the contact points of the spheres results in only a local elimination of the pores. Hence, keeping the fusion temperature to 700 °C or less, it is possible to prepare meso/macroporous monoliths with a specific surface area of 240 m²/g or more with a mesopore volume of around 0.4 cm³/g.

Mercury intrusion porosimetry data shows that the pore size distribution for the monoliths prepared from P123-templated polydisperse particles is bimodal with a macroporous region at 0.1–0.4 μm and a mesoporous region around 10 nm (Figure 4b). We find that the total volume of macropores ($d > 0.1 \mu\text{m}$) decreases continuously with increasing preparation temperature (Table 1), which probably can be related to the temperature-dependent deformation of the mesoporous particles (Figure 2b,c).

The size of the macropores can be tailored by the size and packing of the initial mesoporous powder. An assembly of relatively large CTAB-templated monodisperse mesoporous particles form a mechanically stable meso/macroporous monolith at 750 °C (Figure 4a) that displays a well-defined macropore size distribution between 1 and 4 μm with a total macropore volume of 0.3 cm³/g, Figure 4c. Hence, increasing the average particle size about 10 times resulted in a

hierarchically porous monolith where the pore size of the macropores also increased about 10 times. It is possible to tailor the macroporosity size distribution further by exerting a higher degree of control of the packing of the mesoporous particles. Future work will involve attempts to use colloidal processing and assembly approaches^{36–38} to obtain particle arrays with a long-range order.

The CTAB-templated mesoporous particles also retain the original pore size (21 Å) after pulsed current processing. Hence, even this type of mesoporous materials that are known to display a poorer thermal stability compared to the P123-templated materials can be used to produce monoliths with a well-defined bimodal porosity.^{39–41}

We have evaluated the mechanical stability of the meso/macroporous monoliths, produced from the P123-templated polydisperse particles using the diametral compression test (also known as Brazilian disk test or splitting tensile test) on cylindrical monoliths prepared at different temperatures. This simple test, which is frequently used to characterize powder bodies and composites,⁴² subjects a circular disk to a compressive stress between two diametrically opposed plates

(36) Gates, B. Y. X. *Adv. Mater.* **2000**, *12*, 1329.

(37) Stein, A.; Schroden, R. C. *Curr. Opin. Solid State Mater. Sci.* **2001**, *5*, 553.

(38) Bergstöm, L. In *Handbook of Applied Surface and Colloid Chemistry*; Holmberg, K., Ed.; Wiley & Sons: New York, 2001; pp 201–218.

(39) Zhao, D. Y.; Tian, B. Z.; Liu, X. Y. *Stud. Surf. Sci. Catal.* **2004**, *148*, 139.

(40) Zhao, D. Y.; Huo, Q. S.; Feng, J. L.; Chmelka, B. F.; Stucky, G. D. *J. Am. Chem. Soc.* **1998**, *120*, 6024.

(41) Zhao, D. Y.; Feng, J. L.; Huo, Q. S.; Melosh, N.; Fredrickson, G. H.; Chmelka, B. F.; Stucky, G. D. *Science* **1998**, *279*, 548.

(42) Walker, W. J.; Reed, J. S. *Ceram. Eng. Sci. Proc.* **1993**, *14*, 43.

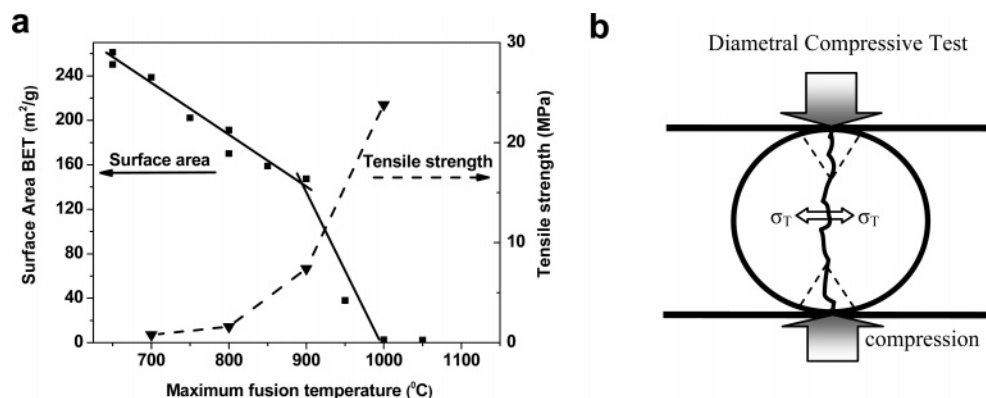


Figure 5. (a) Tensile strength and specific surface area of cylindrical monoliths produced from P123-templated polydisperse particles by pulsed current processing at different temperatures; (b) outline of the tensile strength measurement by diametral compression.

(Figure 5b). The strength of the material can be related to the tensile stress that develops perpendicularly to the loading direction and is proportional to the applied compressive force.⁴³ Figure 5a shows that the tensile strength of the meso/macroporous silica monoliths depends strongly on the fusion temperature (or porosity). Increasing the maximum fusion temperature to 800 °C increases the strength to 1.6 MPa, with only a slight decrease in the specific surface area. Increasing the maximum temperature to 900 °C increases the strength substantially, reaching 7.4 MPa. It should be noted that although there is a substantial collapse of the meso- and macrostructure at this temperature, the specific surface area is close to 150 m²/g and more than 50% of the original macro pore volume remains. There are few studies on the mechanical properties for materials with a hierarchical pore structure.^{44,45} Takahashi and co-workers⁴⁵ found that the bending strength of bimodal silica gel monoliths, prepared from a water–glass solution that is phase separated, varied from 1 to 5 MPa depending on the calcination temperature and the preparation condition. The strength of our monoliths are similar in magnitude,⁴⁶ which suggests that the partial fusion of mesoporous particles creates an interparticle bond that is comparable to a gelled and condensed silica network. The partially fused monoliths have a sufficient strength to allow well-established, so-called green machining techniques, e.g., mechanical polishing, ultrasound milling, and probably also laser cutting, to be used.²⁵ Figure 6 gives an example of a simple shape that has been machined from the dome-shaped monolith prepared at a fusing temperature of 800 °C.

In summary, mechanically stable hierarchically porous silica monoliths, with tunable open macropores and surfactant-templated ordered mesopores, were fabricated by a novel and facile approach. Rapid heating of powder assemblies subjected to a compressive stress results in viscoelastic deformation and partial fusion of the mesoporous silica particles at the contact points. Restricting the maximum

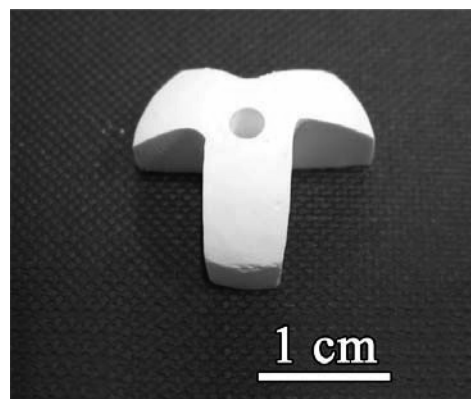


Figure 6. Example of a shape that can be fabricated by machining of a meso/macroporous monolith. The original dome-shaped monolith is depicted in the middle of Figure 2a.

temperature to 750 °C results in monoliths with a bimodal porosity where the mesopores are virtually unaffected by the heating process.

We have demonstrated how the size of the macropores can be controlled by using mesoporous particles of different sizes. It was also demonstrated how monoliths of different shapes could be manufactured by either using dies of various geometries or machining the fabricated monoliths. The combination of an aerosol-assisted continuous scalable production method of mesoporous particles with a rapid technique to produce meso/macroporous monoliths of an arbitrary shape opens up many large-scale applications for advanced materials, e.g., bioseparation and chromatography.

Acknowledgment. This work was supported by the Swedish Science Council (VR). We would like to acknowledge P. Alberius and N. Anderson at The Institute for Surface Chemistry YKI for providing the P123-templated, polydisperse mesoporous particles. We thank Y. Sakamoto, K. Jansson, P. Jansson, D. Salomon, and B. S. Ng for technical assistance and fruitful discussion.

Supporting Information Available: TEM image of P123-templated mesoporous polydisperse particles generated in a two-fluid spray nozzle. SEM image of CTAB-templated monodisperse particles. XRD and nitrogen sorption isotherm data of partially fused particles. This material is available free of charge via the Internet at <http://pubs.acs.org>.

CM061205V

- (43) Timoshenko, S. P.; Goodier, J. N. *Theory of Elasticity*; McGraw-Hill: New York, 1970.
- (44) Martin, J.; Hosticka, B.; Lattimer, C.; Norris, P. M. *J. Non-Cryst. Solids* **2001**, *285*, 222.
- (45) Takahashi, R.; Sato, S.; Sodesawa, T.; Goto, T.; Matsutani, K.; Mikami, N. *Mater. Res. Bull.* **2005**, *40*, 1148.
- (46) Amin, M. C. I.; Fell, J. T. *Drug Dev. Ind. Pharm.* **2002**, *28*, 809 and references there in.